

Lattice instability and superconductivity in the Pb, Sn, and Ba Chevrel phases

J. D. Jorgensen, D. G. Hinks, and G. P. Felcher

Materials Science Division, Argonne National Laboratory, Argonne, Illinois 60439

(Received 10 November 1986)

High-resolution neutron powder diffraction measurements show that sintered samples of PbMo_6S_8 , SnMo_6S_8 , and BaMo_6S_8 all transform from a high-temperature rhombohedral $R\bar{3}$ structure to a low-temperature triclinic $P\bar{1}$ structure, but with a broad temperature range over which both phases are present. The temperature of the structural transition, which may be varied with pressure or composition, is empirically correlated with the superconducting transition temperature T_c .

Over the past ten years numerous authors have reported evidence for a subtle phase transition occurring at temperatures near 100 K in PbMo_6S_8 and SnMo_6S_8 . The experiments which have shown an anomaly in this temperature region include studies of the ^{119}Sn Mössbauer effect,¹⁻³ inelastic neutron scattering (Ref. 4), ^{119}Sn NMR relaxation,⁵ elastic properties,⁶ magnetic susceptibility,^{7,8} resistivity,⁸ specific heat,⁸ x-ray powder diffraction,^{8,9} and neutron powder diffraction.¹⁰ Unfortunately, in every case the observed anomalies have been small and it has been impossible to determine the exact nature of the suspected transition. Evidence for lattice instability in PbMo_6S_8 and SnMo_6S_8 is of particular interest because these two compounds exhibit the highest superconducting transition temperatures $T_c > 14$ K observed in the Chevrel phases. Two recent authors presented models which show a relationship between electronic or structural instability and superconducting behavior in the Chevrel phases with divalent metal cations, $M^{2+}\text{Mo}_6\text{S}_8$ ($M = \text{Pb, Sn, Eu, Ba, Ca, Sr, Yb}$).^{11,12} Johnson, Tarascon, and Sienko suggested a systematic relationship between phase transition temperature (or pressure), superconducting transition temperature, and second ionization potential of the ternary cation.¹¹ However, they define as "phase transition temperature" the temperature of the well-known structural transition to the triclinic $P\bar{1}$ phase of some materials (i.e., $M = \text{Eu, Ba, Ca, Sr}$)¹³⁻¹⁵ and the temperature of the above-mentioned anomaly in other cases (i.e., $M = \text{Pb, Sn, Yb}$). Conversely, Meul concludes that the experimental evidence supports the existence of two transitions in the $M^{2+}\text{Mo}_6\text{S}_8$ Chevrel phases, based on the fact that even in systems such as BaMo_6S_8 , EuMo_6S_8 , and SrMo_6S_8 anomalies in transport and other properties extend well above the triclinic phase transition temperature.^{12,16} Such conclusions bring forth the proposal of an "intermediate" phase. The purpose of this Rapid Communication is to elucidate the nature of this intermediate region and to discuss the observed correlation between structural instability and superconducting behavior in these materials.

The powder samples for this study were synthesized by sintering the elements at high temperature in sealed, evacuated, fused-silica ampoules in quantities of about 15 g each. Neutron powder diffraction data were collected over a range of temperatures by the time-of-flight technique on the Special Environment Powder Diffractometer at the In-

tense Pulsed Neutron Source and the data were analyzed by the Rietveld technique.^{17,18} For BaMo_6S_8 , a triclinic $P\bar{1}$ phase as reported by Baillif, Dunand, Muller, and Yvon¹³ was observed below 175 K. The results of our structural refinements in the $P\bar{1}$ phase have been published elsewhere.¹⁹ Above 350 K, BaMo_6S_8 exhibits a rhombohedral $R\bar{3}$ structure, exactly as was previously seen in PbMo_6S_8 and SnMo_6S_8 above 100 K.¹⁰ Between 350 and 175 K, new Bragg reflections develop as shoulders on many of the $R\bar{3}$ reflections with a pattern for BaMo_6S_8 identical to that previously reported below 100 K for PbMo_6S_8 .¹⁰

In the case of PbMo_6S_8 and SnMo_6S_8 , these new Bragg reflections were originally interpreted as evidence for a modulation of the $R\bar{3}$ structure.¹⁰ (The $R\bar{3}$ peaks persist in the intermediate region, with intensity decreasing with the temperature.) However, a careful analysis of the q dependence of the new Bragg peaks reveals that they cannot be assigned to a modulated $R\bar{3}$ structure. Assuming for simplicity one modulation period Λ in an arbitrary direction, satellites should appear around a peak with lattice spacing d_i at the values of the scattering vector:

$$\mathbf{q} = \left[\frac{2\pi}{d_i} \right] \pm \left[\frac{2\pi}{\Lambda} \right] = \mathbf{q}_{R\bar{3}} \pm \mathbf{q}_M \quad (1)$$

This relation has important consequences even for a powder pattern, which contains diffraction peaks due to all relative orientations of $\mathbf{q}_{R\bar{3}}$ and \mathbf{q}_M . Thus, around the peaks $|q_{h,k,l}|$ and $|q_{2h,2k,2l}|$ of the $R\bar{3}$ structure, one should be able to find satellites displaced with the same $|\Delta q|$. In the PbMo_6S_8 and BaMo_6S_8 data, this is not the case. Instead, all the "modulation" peaks exhibit $|\Delta q| \propto |q|$, which is the signature of a new structure with symmetry lower than $R\bar{3}$. A visual inspection of the diffraction patterns at different temperatures indicates that the modulation pattern is identical to the $P\bar{1}$ pattern at lower temperature.

The presence of two phases ($R\bar{3}$ and $P\bar{1}$) in the intermediate region has been extensively tested by analyzing both the BaMo_6S_8 and PbMo_6S_8 data with a two-phase Rietveld refinement code.²⁰ The refinements included approximately 700 $R\bar{3}$ reflections and 2100 $P\bar{1}$ reflections within the range $0.66 \text{ \AA} < d < 3.1 \text{ \AA}$. In all cases, the positions and intensities of the new peaks were correctly fit,

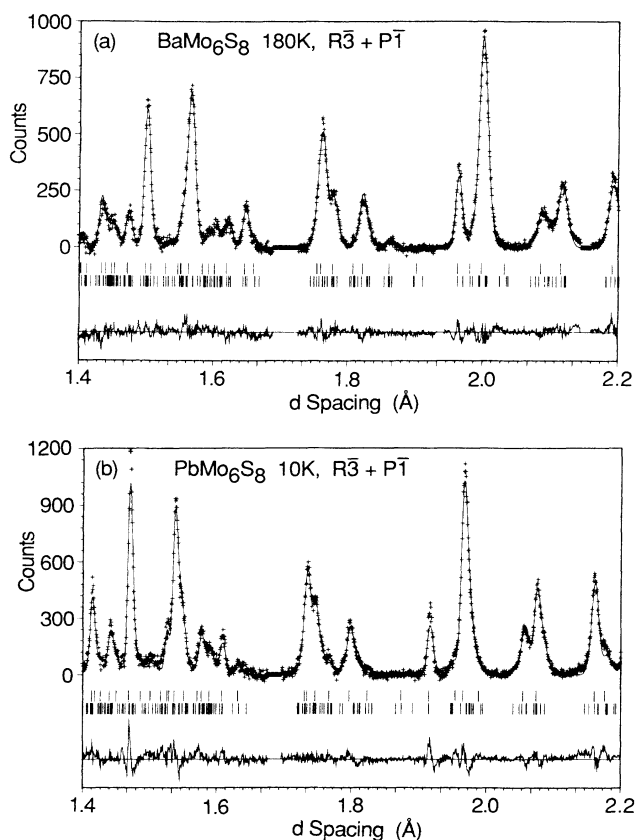


FIG. 1. Portion of the Rietveld refinement profiles based upon a two-phase ($R\bar{3} + P\bar{1}$) model for (a) BaMo_6S_8 at 180 K and (b) PbMo_6S_8 at 10 K. Plus signs (+) are raw data. The continuous line is the calculated profile. At the bottom of the curves, vertical tick marks (|) indicate positions of allowed $R\bar{3}$ (upper tick marks) and $P\bar{1}$ (lower tick marks) reflections.

as shown for small regions of refined data in Fig. 1. Two-phase refinements were not attempted for our SnMo_6S_8 data because the observed new reflections are considerably less pronounced in that case.

The refined $R\bar{3}$ and $P\bar{1}$ lattice constants in the two-phase region for BaMo_6S_8 at 180 K and PbMo_6S_8 at 10 K are given in Table I. In both cases, the triclinic cell volume is slightly (less than 0.5%) larger than the rhombohedral cell volume, consistent with the fact that the

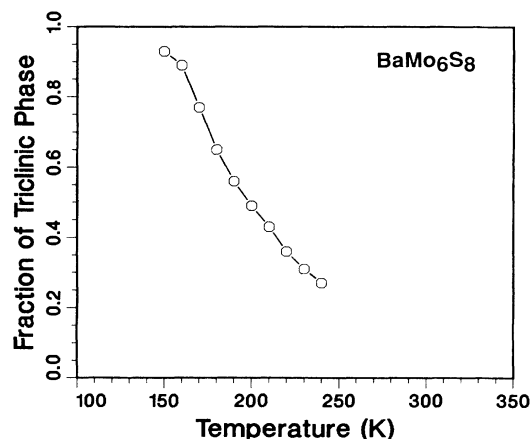


FIG. 2. Fraction of the sample which is in the triclinic phase vs temperature for BaMo_6S_8 .

rhombohedral cell is favored at high pressure. The relative fraction of the $R\bar{3}$ and $P\bar{1}$ phases as a function of temperature for BaMo_6S_8 is shown in Fig. 2. The behavior is analogous for PbMo_6S_8 , where at 10 K the sample studied in this experiment is about 70% triclinic.

The onset of the two-phase region corresponds to the "upper" transition proposed by Meul¹² and the experimental anomaly reported by numerous other authors. The onset temperature is observed in neutron diffraction as a change in the sign of the hexagonal c -axis thermal expansion when data are refined in an $R\bar{3}$ model. The results reported in Fig. 3 for PbMo_6S_8 , SnMo_6S_8 , and BaMo_6S_8 suggest approximate onset temperatures of about 110, 140, and 350 K, respectively. These onset temperatures are undoubtedly sample dependent, as is typical of two-phase behavior associated with first-order transitions.

Based on these observations, a generalized phase diagram which approximately describes the structural behavior of the $M^{2+}\text{Mo}_6\text{S}_8$ Chevrel phases is proposed in Fig. 4. The vertical lines, labeled for each compound, represent the zero pressure axes for the various compounds; i.e., for a given compound, pressure is zero at this point and increases to the right according to the scale shown in the figure. Figure 4 also illustrates the existence of a correlation between unit cell volumes (which scale with the ionic radius of the M^{2+} ion) and the positions of the zero pressure axes in the phase diagram.

TABLE I. Rhombohedral $R\bar{3}$ and triclinic $P\bar{1}$ lattice constants in the two-phase region for BaMo_6S_8 at 180 K and PbMo_6S_8 at 10 K.

	BaMo_6S_8 180 K		PbMo_6S_8 10 K	
	$R\bar{3}$	$P\bar{1}$	$R\bar{3}$	$P\bar{1}$
a (Å)	6.6446(3)	6.6795(15)	6.5273(2)	6.5759(9)
b (Å)		6.6551(15)		6.5383(9)
c (Å)		6.6067(12)		6.4948(8)
α (deg)	88.642(4)	88.254(18)	89.066(3)	88.516(12)
β (deg)		88.846(16)		89.604(11)
γ (deg)		88.878(17)		89.298(13)
V (Å ³)	293.12(3)	293.44(16)	277.99(2)	279.12(4)

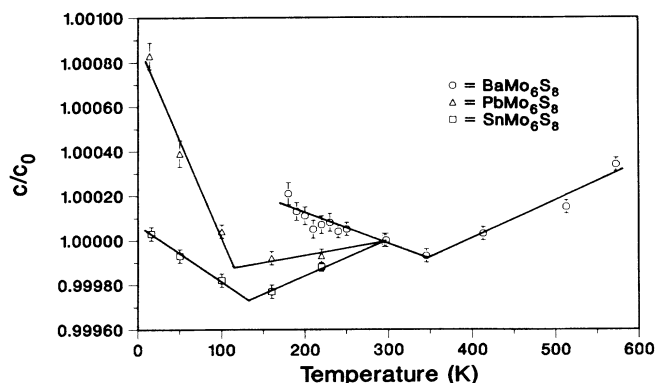


FIG. 3. Hexagonal c -axis lattice constants, based on Rietveld refinement in $R\bar{3}$ symmetry, vs temperature for BaMo_6S_8 , PbMo_6S_8 , and SnMo_6S_8 . c_0 is the room temperature value [$c_0(\text{BaMo}_6\text{S}_8) = 11.7765(4)$ Å, $c_0(\text{PbMo}_6\text{S}_8) = 11.4896(3)$ Å, $c_0(\text{SnMo}_6\text{S}_8) = 11.3918(2)$ Å].

An empirical correlation exists between the superconducting properties of the $M^{2+}\text{Mo}_6\text{S}_8$ Chevrel phases where the metal cation occupies the origin position (e.g., $M = \text{Pb}, \text{Sn}, \text{Eu}, \text{Ba}, \text{Yb}$, etc.) and the proposed structural phase diagram. The compounds with a stable $P\bar{1}$ structure at atmospheric pressure (i.e., EuMo_6S_8 and BaMo_6S_8) are not superconducting. For the others, when superconductivity is not perturbed by impurity defects, the highest T_c 's always occur in the two-phase region adjacent to the $P\bar{1}$ transition line. As one moves away from this line, for example, by applying pressure to PbMo_6S_8 or SnMo_6S_8 , T_c decreases.^{21,22} The effects of pressure on T_c are among the largest reported for any compounds. YbMo_6S_8 , which shows no mixed-phase behavior at low temperature in our neutron diffraction experiments,²³ has a lower T_c —approximately 10 K. Analogous behavior is observed in EuMo_6S_8 : As pressure is increased, there is a sudden onset of superconductivity with $T_c = 11.8$ K upon crossing the triclinic phase line, but a further increase in pressure decreases T_c .²⁴ The onset of pressure-induced superconductivity in BaMo_6S_8 was originally reported to be at 19 kbar.²⁵ The two-phase behavior could explain initial reports that superconductivity in BaMo_6S_8 (based on observations under nonhydrostatic conditions at 15 kbar) is non-bulk.²⁶ More recent data show an onset of superconductivity in BaMo_6S_8 at 25 kbar with a T_c of 14 K.²⁷ These observations, thus, show that high T_c 's in the $M^{2+}\text{Mo}_6\text{S}_8$ Chevrel phases are related in a systematic way to the lattice instability which drives the triclinic phase transition.

These conclusions have several implications for understanding the observed superconductivity behavior in the

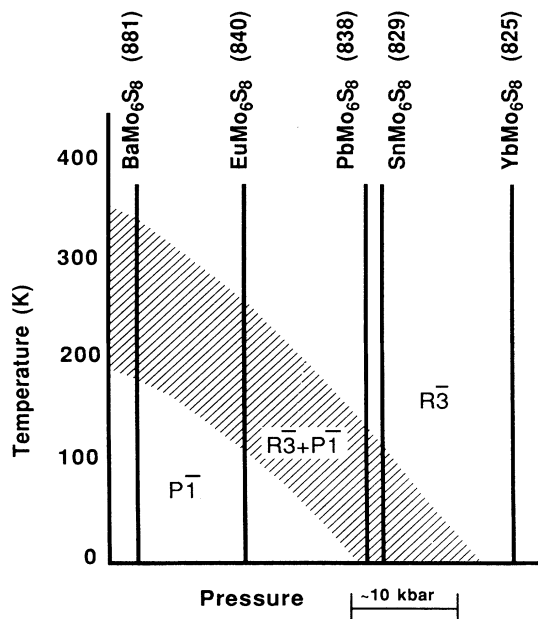


FIG. 4. Generalized structural phase diagram for Chevrel phases with divalent tenary metal cations. Vertical lines are the zero pressure axes for the compounds indicated. Numbers in parentheses are the hexagonal unit cell volumes (at room temperature and zero pressure) for the compounds indicated.

Chevrel phases. Since PbMo_6S_8 and SnMo_6S_8 already lie directly adjacent to the triclinic phase line, attempts to achieve T_c 's higher than 14 K (e.g., by alloying) may never succeed unless the transition to the triclinic phase can be suppressed. Furthermore, existing samples of PbMo_6S_8 and SnMo_6S_8 may contain large fractions of nonsuperconducting ($P\bar{1}$) material. Such a hypothesis could explain the failure to achieve the expected large critical current densities in wires and films of these materials.²⁸ In summary, many of the properties of these compounds hitherto observed are undoubtedly related to the presence of two coexisting phases. The next experimental challenge is to produce samples with sharp first-order transitions so that the intrinsic behavior can be studied.

This work was supported by the U.S. Department of Energy, Basic Energy Sciences-Materials Sciences, under Contract No. W-31-109-ENG-38. The authors wish to thank Daniel L. Decker for fruitful discussions, and Y. S. Yao, R. P. Guertin, S. Bloom, M. Kuric, D. W. Capone II, and D. G. Hinks for making available their unpublished results for superconductivity in BaMo_6S_8 under pressure.

¹C. W. Kimball, L. Weber, G. Van Landuyt, F. Y. Fradin, B. D. Dunlap, and G. K. Shenoy, *Phys. Rev. Lett.* **36**, 412 (1976).

²J. Bolz, J. Hauck, and F. Pobell, *Z. Phys. B* **25**, 351 (1976).

³H. A. Wagner and H. C. Freyhardt, in *Superconductivity in d- and f-Band Metals*, edited by W. Buckel and W. Weber (Academic, New York, 1982), pp. 197–200.

⁴S. D. Bader, G. S. Knapp, S. K. Sinha, P. Schweiss, and B. Renker, *Phys. Rev. Lett.* **37**, 344 (1976).

⁵N. E. Alekseevskii and E. G. Nikolaev, *Pis'ma Zh. Eksp. Teor. Fiz.* **34**, 350 (1981) [*JETP Lett.* **34**, 333 (1981)].

⁶A. S. Balankin, Yu. F. Bychkov, and A. M. Kharchenkov, *Pis'ma Zh. Tekh. Fiz.* **11**, 72 (1985) [*Sov. Tech. Phys. Lett.* **11**, 72 (1985)].

- 11, 28 (1985)].
- ⁷M. E. Reeves, W. M. Miller, and D. M. Ginsberg, *J. Low Temp. Phys.* **59**, 509 (1985).
- ⁸A. D. Shevchenko, O. V. Aleksandrov, S. V. Drozdova, G. A. Kalyuzhnaya, K. V. Kiseleva, V. F. Primachenko, N. V. Shevchuk, and V. E. Yachmenev, *Fiz. Nizk. Temp.* **8**, 688 (1982) [*Sov. J. Low Temp. Phys.* **8**, 342 (1982)].
- ⁹M. Marezio, P. D. Dernier, J. P. Remeika, E. Corenzwit, and B. T. Matthias, *Mater. Res. Bull.* **8**, 657 (1973).
- ¹⁰J. D. Jorgensen and D. G. Hinks, *Solid State Commun.* **53**, 289 (1985).
- ¹¹D. C. Johnson, J. M. Tarascon, and M. J. Sienko, *Inorg. Chem.* **24**, 2598 (1985).
- ¹²H. W. Meul, *Helv. Phys. Acta* **59**, 417 (1986).
- ¹³R. Baillif, A. Dunand, J. Muller, and K. Yvon, *Phys. Rev. Lett.* **47**, 672 (1981).
- ¹⁴B. Lachal, R. Baillif, A. Junod, and J. Muller, *Solid State Commun.* **45**, 849 (1983).
- ¹⁵R. Baillif, A. Junod, B. Lachal, J. Muller, and K. Yvon, *Solid State Commun.* **40**, 603 (1981).
- ¹⁶C. Rossel, M. B. Maple, H. W. Meul, Ø. Fischer, X. J. Zhang, and N. P. Ong, *Physica B* **135**, 381 (1985).
- ¹⁷J. D. Jorgensen and J. Faber, Jr., in *Proceedings of the Sixth Meeting of the International Collaboration on Advanced Neutron Sources*, Argonne National Laboratory Report No. ANL-82-80, 1983 (unpublished), pp. 105–114.
- ¹⁸R. B. Von Dreele, J. D. Jorgensen, and C. G. Windsor, *J. Appl. Crystallogr.* **15**, 27 (1982).
- ¹⁹J. D. Jorgensen and D. G. Hinks, *Physica B* **136**, 485 (1986).
- ²⁰F. J. Rotella (unpublished).
- ²¹R. N., Shelton, A. C. Lawson, and D. C. Johnson, *Mater. Res. Bull.* **10**, 297 (1975).
- ²²D. W. Capone II, R. P. Guertin, S. Foner, D. G. Hinks, and H. C. Li, *Phys. Rev. B* **29**, 6375 (1984).
- ²³D. W. Capone II, R. P. Guertin, S. Foner, D. G. Hinks, and H. C. Li, *Phys. Rev. Lett.* **51**, 601 (1983).
- ²⁴J. D. Jorgensen, D. G. Hinks, D. R. Noakes, P. J. Viccaro, and G. K. Shenoy, *Phys. Rev. B* **27**, 1465 (1983), and additional unpublished results.
- ²⁵W. Kalsbach, *Structural Phase Transitions and Pressure-Induced Superconductivity of Molybdenum Cluster Compounds*, *Berichte Kernforschungsanlage, Juelich 1984*, Report No. Juel-1921, 1984 (unpublished).
- ²⁶P. M. Hor, M. K. Wu, T. H. Lin, X. Y. Shao, X. C. Jin, and C. W. Chu, *Solid State Commun.* **44**, 1605 (1982).
- ²⁷Y. S. Yao, R. P. Guertin, S. Bloom, M. Kuric, D. W. Capone II, and D. G. Hinks (unpublished).
- ²⁸M. Decroux and Ø. Fischer, in *Superconductivity in Ternary Compounds*, *Topics in Current Physics*, Vol. 34, edited by M. B. Maple and Ø. Fischer (Springer-Verlag, Berlin, 1982), pp. 57–98.